Geomechanics and Engineering, *Vol. 24, No. 4 (2021) 371-388*
DOI: https://doi.org/10.12989/gae.2021.24.4.371

Nonlinear flexibility-based beam element on Winkler-Pasternak foundation

Worathep Sae-Long[1], Suchart Limkatanyu*[2], Chayanon Hansapinyo[3], Woraphot Prachasaree[2], Jaroon Rungamornrat[4] and Minho Kwon[5]

[1]Department of Civil Engineering, School of Engineering, University of Phayao, Phayao 56000, Thailand
[2]Department of Civil Engineering, Faculty of Engineering, Prince of Songkla University, Songkhla 90110, Thailand
[3]Excellence Center in Infrastructure and Transportation Engingeering (ExCITE), Department of Civil Engineering, Chiang Mai University, Chiang Mai 50200, Thailand
[4]Applied Mechanics and Structures Research Unit, Department of Civil Engineering, Faculty of Engineering, Chulalongkorn University, Bangkok 10330, Thailand
[5]Department of Civil Engineering, ERI, Gyeongsang National University, Jinju 660-701, South Korea

(Received May 10, 2020, Revised January 30, 2021, Accepted January 31, 2021)

Abstract. A novel flexibility-based beam-foundation model for inelastic analyses of beams resting on foundation is presented in this paper. To model the deformability of supporting foundation media, the Winkler-Pasternak foundation model is adopted. Following the derivation of basic equations of the problem (strong form), the flexibility-based finite beam-foundation element (weak form) is formulated within the framework of the matrix virtual force principle. Through equilibrated force shape functions, the internal force fields are related to the element force degrees of freedom. Tonti's diagrams are adopted to present both strong and weak forms of the problem. Three numerical simulations are employed to assess validity and to show effectiveness of the proposed flexibility-based beam-foundation model. The first two simulations focus on elastic beam-foundation systems while the last simulation emphasizes on an inelastic beam-foundation system. The influences of the adopted foundation model to represent the underlying foundation medium are also discussed.

Keywords: flexibility-based formulation; beam element; Winkler-Pasternak foundation; soil-structure interaction; virtual force principle; finite element; nonlinear analysis

1. Introduction

In engineering and applied science, the interactive mechanism between structural members (e.g., beam, plate, shell) and their contacting foundation medium has found a wide spectrum of applications (He and Kwan 2001, Civalek and Ozturk 2010, Gangadean *et al.* 2010, Shokrieh and Heidari-Rarani 2011, Limkatanyu *et al.* 2012a, Kim *et al.* 2014, Khemis *et al.* 2016, Ebrahimi and Barati 2017, Zarepour *et al.* 2017, Demir *et al.* 2018, Bohlooly and Fard 2019, Jamil and Admah 2019). Several analytical models have been proposed to study this interaction mechanism with varying levels of mathematical sophistication in representing the contacting foundation medium (Selvadurai 1979). A simple model often referred to as "mechanical subgrade model" is to consider the contacting foundation medium as a bed of single or combined structural components (e.g., spring, shear-layer, membrane) while a rigorous model often referred to as "continuum model" is to represent the contacting foundation medium by a semi-infinite continuum body (Mindlin 1936). The pros and cons of these two extremes were thoroughly discussed in Selvadurai (1979) and Dutta and Roy (2002). Even though the continuum model is more realistic and can provide detailed analysis results, its use among practicing engineers is still limited due to its complexity and high computational effort. On the other hand, the mechanical subgrade model is very popular in practicing-engineering community due to its simplicity and computational efficiency. The Winkler foundation model (Winkler 1867) is the most rudimentary mechanical subgrade model in which a set of continuously smeared independent springs is adopted to represent the contacting foundation medium. Even though the Winkler foundation model behaves in a peculiar manner for some beam-foundation systems as pointed out in Kerr (1964), a countless list of analytical and numerical beam-foundation models have been formulated using this foundation model due to its simplified representation of the foundation-medium response (Hetenyi 1946, Eisenberger and Yankelevsky 1985, Zhang *et al.* 2009, Limkatanyu *et al.* 2012a, b, Raychowdhury and Jindal 2014, Kim *et al.*, 2015). The rudimentary flaw inherent in the Winkler foundation model is associated with the non-interconnected nature of foundation-spring bed, thus completely neglecting the cohesive bonds (continuous nature) between foundation-medium.

To consider the continuous nature of the foundation medium, the Winkler foundation model has been enhanced with different embedded structural components to introduce coupled effects between continuously smeared independent springs (Horvath and Colasanti 2011), thus resulting in several forms of the enhanced Winkler foundation model. More detailed discussions on this enhanced Winkler foundation model are found and thoroughly discussed in

*Corresponding author, Professor, Ph.D.
E-mail: suchart.l@psu.ac.th

http://www.techno-press.org/?journal=gae&subpage=7
ISSN: 2005-307X (Print), 2092-6219 (Online)

Dutta and Roy (2002). In the present work, the improved Winkler foundation model proposed by Pasternak (1954) is of particular interest. This foundation model is called the "Winkler-Pasternak" foundation model. An incompressible shear layer is inserted between the beam and the Winkler foundation springs in this foundation model. Several beam elements on Winkler-Pasternak foundation have been formulated by various researchers using analytically derived displacement shape functions (Zhaohua and Cook 1983, Gülkan and Alemdar 1999) or assumed displacement shape functions (Zhaohua and Cook 1983, Teodoru and Musat 2010). However, all aforementioned beam elements are valid only for elastic systems. Along with the recently adopted performance-based design and assessment methodology (ICC 2012), inelastic responses of beam-foundation systems are essential in analyzing, designing, and assessing both existing and newly constructed structures under extreme loadings. Unfortunately, only few inelastic Winkler-Pasternak based beam-foundation elements have been formulated in the literature using the finite element technique (Mullapudi and Ayoub 2010, Patil *et al.* 2012, Limkatanyu *et al.* 2015) and boundary element technique (Sapountzakis and Kampitsis 2013). Regarding this issue, there is a research opportunity to develop a more computationally efficient nonlinear beam-foundation model.

In the present work, a newly proposed model for inelastic analysis of beam-foundation systems is constructed within the framework of flexibility-based finite element formulation. Up to date, the flexibility-based finite element formulation has gained growing interests in establishing a more efficient computational platform for inelastic analysis of structures and has been proved to remedy several flaws inherent in the standard stiffness-based finite element formulation (Spacone *et al.* 1996a, Neuenhofer and Filippou 1997, Salari *et al.* 1998, Limkatanyu and Spacone 2002a, Limkatanyu and Spacone 2006, Jafari *et al.* 2009, Zendaoui *et al.* 2016, Feng *et al.* 2019). The enhanced performance of the flexibility-based model is due to the merits of employed force shape functions. These merits stem from two main observations; (a) in certain structural elements, the internal force distributions along the element length can be determined exactly, thus resulting in the "exact" finite element model; and (b) along the element length, the internal force distributions are generally smoother than the internal deformation distributions which drastically vary across the inelastic regions (e.g., plastic hinge). For the present beam-foundation system, the determination of internal force distributions is not straightforward due to its internally statically indeterminate feature. Consequently, certain internal force distribution has to be assumed, thus resulting in the internally statically determinate beam-foundation system. This internal-force determination procedure follows those employed by Limkatanyu and Spacone (2002a) for the reinforced concrete beam with bond interfaces; and by Limkatanyu and Spacone (2006) for the beam resting on Winkler foundation.

The presentation of the paper is in the following order. First, the system basic equations (strong form) are presented. Then, the flexibility-based beam-foundation model (weak form) is formulated within the framework of the matrix virtual force principle. The general procedure of both strong and weak forms of the problem are compactly depicted in Tonti's diagrams. The derivation of equilibrated force shape functions and the general procedure for the element state determination are presented as well. Assessment of model validity and demonstration of model effectiveness are finally shown via three numerical simulations. The first two simulations focus on elastic beam-foundation systems and show the model accuracy in representing responses at both global and local levels. The last simulation emphasizes on an inelastic beam-foundation system. Convergence studies of the proposed model are carried out at both global and local levels and its accuracy and efficiency are confirmed by comparing their global and local responses with those obtained with stiffness-based models. Effects of different foundation models on the system responses are also addressed. All mathematical symbols in this paper are formulated from Mathematica software package (Wolfram 1992).

2. Basic equations of beams on Winkler-Pasternak foundation (strong form)

2.1 Equilibrium

A Winkler-Pasternak based beam-foundation system is shown in Fig. 1 and the free body diagram of its differential segment consists of two parts. The first shown in Fig. 2(a) presents the beam differential segment interacting with an underlying shear layer while the second shown in Fig. 2(b) presents the shear-layer differential segment sandwiched between the beam and the Winkler-spring bed. Following the infinitesimal deformation hypothesis, all of equilibrium equations are written with respect to the undeformed configuration. Considering moment and vertical equilibriums of the beam component of Fig. 2(a) yields the following expressions:

$$V_B(x) - \frac{dM_B(x)}{dx} = 0 \tag{1}$$

$$-\frac{dV_B(x)}{dx} - D_2(x) + p_y(x) = 0 \tag{2}$$

with $V_B(x)$ being the beam-section shear force; $M_B(x)$ being the beam-section bending moment; $D_2(x)$ being the foundation-interactive force acting at the beam bottom face; and $p_y(x)$ being the transverse distributed load.

Following the Euler-Bernoulli beam theory adopted in the present work, the beam-section shear force $V_B(x)$ plays no role in the model formulation. As a result, Eqs. (1) and (2) are written together as:

$$D_2(x) + \frac{d^2M_B(x)}{dx^2} - p_y(x) = 0 \tag{3}$$

Vertical equilibrium of the shear-layer component of Fig. 2(b) leads to the following expression:

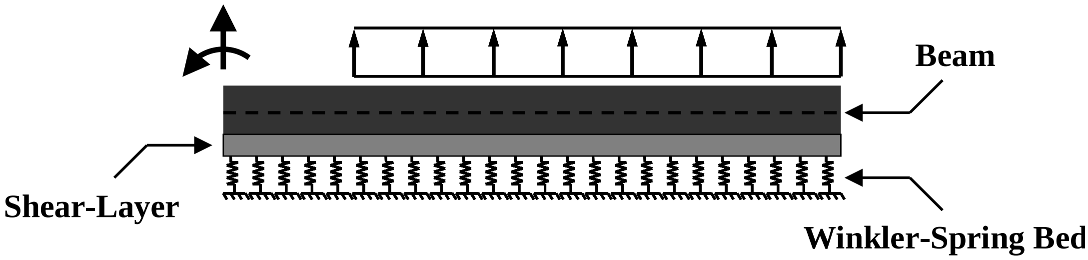

Fig. 1 A beam on Winkler-Pasternak foundation

$$D_2(x) - D_1(x) - \frac{dV_S(x)}{dx} = 0 \tag{4}$$

where $D_1(x)$ is the Winkler-foundation interactive force acting at the shear-layer bottom face and $V_s(x)$ is the shear-layer section shear force. Eq. (4) presents the equilibrium relation between the foundation internal forces ($D_1(x)$, $D_2(x)$, and $V_s(x)$) and is also observed by Ghosh *et al.* (2017).

Substituting Eqs. (4) into (3) leads to one single expression as:

$$\frac{d^2M_B(x)}{dx^2} + \frac{dV_S(x)}{dx} + D_1(x) - p_y(x) = 0 \tag{5}$$

Eq. (5) presents the governing equilibrium equation for the problem of Winkler-Pasternak based beam-foundation systems and is expressed in the matrix form as:

$$\mathbf{L}_B^T\mathbf{D}_B(x) + \mathbf{L}_F^T\mathbf{D}_F(x) - \mathbf{p}(x) = \mathbf{0} \tag{6}$$

with $\mathbf{D}_B(x) = \{M_B(x)\}^T$ being the beam-section force vector; $\mathbf{D}_F(x) = \{D_1(x) \quad V_S(x)\}^T$ being the foundation-section force vector; and $\mathbf{p}(x) = \{p_y(x)\}^T$ being the element force vector. The beam $\mathbf{L}_B$ and foundation $\mathbf{L}_F$ differential operators are expressed as:

$$\mathbf{L}_B = \left[\frac{d^2}{dx^2}\right]; \text{ and } \mathbf{L}_F = \begin{bmatrix} 1 \\ \dfrac{d}{dx} \end{bmatrix} \tag{7}$$

From Eq. (5), the beam-foundation system is inherently statically indeterminate. At any system section, there are 3 unknown internal forces ($M_B(x)$, $D_1(x)$, and $V_s(x)$) while only one equilibrium condition of Eq. (5) is accessible. Consequently, only equilibrium consideration is not sufficient to determine all unknown internal forces. This issue is to be discussed subsequently in the paper. Furthermore, the eliminated beam-section shear force $V_B(x)$ and the eliminated foundation interactive force $D_2(x)$ can be retrieved from Eqs. (2) and (4), respectively once all remaining unknown internal forces ($M_B(x)$, $D_1(x)$, and $V_s(x)$) are obtained.

2.2 Compatibility

At any section of the beam-foundation system, the beam and foundation deformations and the beam transverse displacement are related through the sectional compatibility conditions. The beam-section deformation vector $\mathbf{d}_B(x)$ collects the beam-section bending curvature $\kappa_B(x)$ as:

$$\mathbf{d}_B(x) = \{\kappa_B(x)\}^T \tag{8}$$

The beam displacement vector $\mathbf{u}(x)$ collects the beam transverse displacement $v_B(x)$ as:

$$\mathbf{u}(x) = \{v_B(x)\}^T \tag{9}$$

Following the infinitesimal-deformation hypothesis, the compatibility relation between the beam-section bending curvature $\kappa_B(x)$ and the beam transverse displacement $v_B(x)$ as:

$$\kappa_B(x) = \frac{d^2v_B(x)}{dx^2} \tag{10}$$

Eq. (10) can be expressed in the matrix form as:

$$\mathbf{d}_B(x) = \mathbf{L}_B\mathbf{u}(x) \tag{11}$$

The Winkler-spring deformation $v_s(x)$ and the shear-layer section shear strain $\gamma_s(x)$ define foundation deformations. Following the Winkler-Pasternak foundation model, the foundation compatibility conditions are:

$$v_S(x) = v_B(x); \quad \gamma_S(x) = \frac{dv_B(x)}{dx} \tag{12}$$

Eq. (12) can be written in the matrix form as:

$$\mathbf{d}_F(x) = \mathbf{L}_F\,\mathbf{u}(x) \tag{13}$$

with $\mathbf{d}_F(x) = \{v_S(x) \quad \gamma_S(x)\}^T$.

Eqs. (11) and (13) define governing compatibility equations for the Winkler-Pasternak based beam-foundation system. Furthermore, it is observed that the dualism between equilibrium and compatibility relations is confirmed by comparing Eq. (6) with Eqs. (11) and (13).

2.3 Sectional force-deformation relations

In the present study, the sectional constitutive laws can be expressed in consistent linearized incremental matrix forms as:

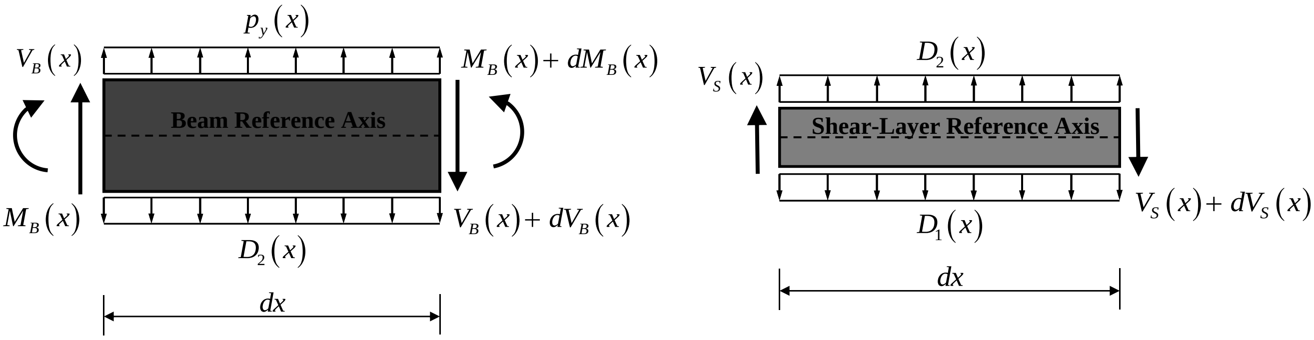

(a) Beam (b) Shear layer

Fig. 2 A differential segment cut from the beam and shear layer

$$\mathbf{D}_B(x)=\mathbf{D}_B^0(x)+\mathbf{k}_B^0(x)\Delta\mathbf{d}_B(x);\quad \mathbf{D}_F(x)=\mathbf{D}_F^0(x)+\mathbf{k}_F^0(x)\Delta\mathbf{d}_F(x) \tag{14}$$

with $\mathbf{D}^0{}_B(x)$ and $\mathbf{D}^0{}_F(x)$ being the initial beam-section and foundation forces, respectively; $\mathbf{k}^0{}_B(x)$ being the beam-section tangent stiffness matrix; and $\mathbf{k}^0{}_F(x)$ being the foundation tangent stiffness matrix.

The consistent inverse of Eq. (14) is required in the flexibility-based finite element formulation and can be expressed as:

$$\mathbf{d}_B(x)=\mathbf{d}_B^0(x)+\mathbf{f}_B^0(x)\Delta\mathbf{D}_B(x);\quad \mathbf{d}_F(x)=\mathbf{d}_F^0(x)+\mathbf{f}_F^0(x)\Delta\mathbf{D}_F(x) \tag{15}$$

with $\mathbf{d}^0{}_B(x)$ and $\mathbf{d}^0{}_F(x)$ being the initial beam-section and foundation deformations, respectively; $\mathbf{f}^0{}_B(x)$ being the beam-section tangent flexibility matrix; and $\mathbf{f}^0{}_F(x)$ being the foundation tangent flexibility matrix.

For the problem of Winkler-Pasternak based beam-foundation systems, governing equations comprised of equilibrium condition (Eq. (6)), compatibility conditions (Eqs. (11) and (13)), and constitutive relation (Eq. (14)) can be compactly presented in the classical Tonti's diagram of Fig. 3 (Tonti 1976). To envisage the whole picture of finite element formulation process, this diagram is to be modified later.

3. Flexibility-based finite element formulation of beams on Winkler-Pasternak foundation (weak form)

3.1 Formulation

The Winkler-Pasternak based beam-foundation element proposed herein is constructed within the framework of flexibility-based finite element formulation. The root of the proposed model stems from the composite beam element with deformable shear connectors (Salari *et al.* 1998), the reinforced concrete frame element with bond-interfaces (Limkatanyu and Spacone 2002a), and the beam resting on Winkler foundation (Limkatanyu and Spacone 2006).

In the flexibility-based finite element model, the element sectional forces $\mathbf{D}_B(x)$, $\mathbf{D}_F(x)$ serves as primary variables and can be related to the element nodal forces through equilibrated force shape functions. The derivation of such force shape functions is associated with enforcing the system equilibrium condition of Eq. (6) and will be discussed subsequently in the paper. Therefore, the system equilibrium condition of Eq. (6) is enforced in the strong sense. In opposition, the beam-section compatibility of Eq. (11) and foundation compatibility of Eq. (13) are satisfied in the weak sense. In the modified Tonti's diagram of Fig. 4, general framework of the flexibility-based formulation of the proposed beam-foundation model is summarized.

The weighted residual statement of Eqs. (11) and (13) is expressed as:

$$\int_L \delta\mathbf{D}_B^T(x)\left[\mathbf{d}_B(x)-\mathbf{L}_B\mathbf{u}(x)\right]dx+\int_L \delta\mathbf{D}_F^T(x)\left[\mathbf{d}_F(x)-\mathbf{L}_F\mathbf{u}(x)\right]dx=0 \tag{16}$$

where $\delta\mathbf{D}_B(x)$ and $\delta\mathbf{D}_F(x)$ represent statically admissible virtual beam-section and foundation-interface force fields, respectively. Substituting the linearized deformation-force relations of Eqs. (15) into (16) leads to:

$$\int_L \delta\mathbf{D}_B^T(x)\left[\mathbf{d}_B^0(x)+\mathbf{f}_B^0(x)\Delta\mathbf{D}_B(x)-\mathbf{L}_B\mathbf{u}(x)\right]dx + \int_L \delta\mathbf{D}_F^T(x)\left[\mathbf{d}_F^0(x)+\mathbf{f}_F^0(x)\Delta\mathbf{D}_F(x)-\mathbf{L}_F\mathbf{u}(x)\right]dx=0 \tag{17}$$

Applying integration by parts to Eq. (17) moves the differential operators $\mathbf{L}_B$ and $\mathbf{L}_F$ from the displacement vector $\mathbf{u}(x)$ to the virtual force vectors $\delta\mathbf{D}_B(x)$ and $\delta\mathbf{D}_F(x)$ and leads to the following virtual force expression:

$$\begin{aligned}&\int_L \delta\mathbf{D}_B^T(x)\mathbf{f}_B^0(x)\Delta\mathbf{D}_B(x)\,dx+\int_L \delta\mathbf{D}_F^T(x)\mathbf{f}_F^0(x)\Delta\mathbf{D}_F(x)\,dx\\&+\int_L \delta\mathbf{D}_B^T(x)\mathbf{d}_B^0(x)\,dx+\int_L \delta\mathbf{D}_F^T(x)\mathbf{d}_F^0(x)\,dx\\&=\delta\mathbf{P}^T\mathbf{U}+\int_L \mathbf{u}(x)\left[\underbrace{\mathbf{L}_B^T\delta\mathbf{D}_B(x)+\mathbf{L}_F^T\delta\mathbf{D}_F(x)}_{\delta\mathbf{p}(x)}\right]dx\end{aligned} \tag{18}$$

where $\delta\mathbf{P}^T\mathbf{U}$ are the boundary terms associated with integration by parts and represents the external virtual work done by the virtual element nodal forces $\delta\mathbf{P}$ on the element nodal displacements $\mathbf{U}$. It can clearly be observed that Eq. (18) presents the virtual force statement of the problem. Enforcing the equilibrium condition of Eq. (6) and arbitrarily selecting the virtual element distributed load vector $\delta\mathbf{P}(x)=0$, Eq. (18) can be simplified in the matrix form as:

$$\int_L \begin{Bmatrix} \delta\mathbf{D}_B(x) \\ \delta\mathbf{D}_F(x) \end{Bmatrix}^T \begin{bmatrix} \mathbf{f}_B^0(x) & \mathbf{0} \\ \mathbf{0} & \mathbf{f}_F^0(x) \end{bmatrix} \begin{Bmatrix} \Delta\mathbf{D}_B(x) \\ \Delta\mathbf{D}_F(x) \end{Bmatrix} dx = \delta\mathbf{P}^T\mathbf{U} - \int_L \begin{Bmatrix} \delta\mathbf{D}_B(x) \\ \delta\mathbf{D}_F(x) \end{Bmatrix}^T \begin{Bmatrix} \mathbf{d}_F^0(x) \\ \mathbf{d}_F^0(x) \end{Bmatrix} dx \quad (19)$$

To gain the discrete form of Eq. (19), the beam-section force $\mathbf{D}_B(x)$ and the foundation-interactive force $\mathbf{D}_F(x)$ are interpolated in terms of the element nodal variables using equilibrated force shape functions. In the present work, the element nodal variables consist of the element nodal forces $\mathbf{P}$ and the foundation-interactive forces $\mathbf{P}_F$ at the selected reference points along the element length. Thus, the interpolation expression between the internal forces ($\mathbf{D}_B(x)$ and $\mathbf{D}_F(x)$) and the nodal forces ($\mathbf{P}$ and $\mathbf{P}_F$) is:

$$\begin{Bmatrix} \mathbf{D}_B(x) \\ \mathbf{D}_F(x) \end{Bmatrix} = \begin{bmatrix} \mathbf{N}_{BB}(x) & \mathbf{N}_{BF}(x) \\ \mathbf{N}_{FB}(x) & \mathbf{N}_{FF}(x) \end{bmatrix} \begin{Bmatrix} \mathbf{P} \\ \mathbf{P}_F \end{Bmatrix} \quad (20)$$

where $\mathbf{N}_{BB}(x)$ and $\mathbf{N}_{BF}(x)$ contain the beam-section force shape functions associated with the element nodal forces $\mathbf{P}$ and the reference foundation-interactive forces $\mathbf{P}_F$, respectively; and $\mathbf{N}_{FB}(x)$ and $\mathbf{N}_{FF}(x)$ collect the foundation-interactive force shape functions associated with the element nodal forces $\mathbf{P}$ and the reference foundation-interactive forces $\mathbf{P}_F$, respectively. The derivation of these force shape functions is to be presented in a subsequent subsection.

Substituting Eqs. (20) into (19) and accounting for the arbitrariness of $\delta\mathbf{P}$ and $\delta\mathbf{P}_F$ lead to the following element flexibility expression:

$$\begin{bmatrix} \mathbf{F}_{BB}^0(x) & \mathbf{F}_{BF}^0(x) \\ \mathbf{F}_{FB}^0(x) & \mathbf{F}_{FF}^0(x) \end{bmatrix} \begin{Bmatrix} \Delta\mathbf{P} \\ \Delta\mathbf{P}_F \end{Bmatrix} = \begin{Bmatrix} \mathbf{U}-\mathbf{r}^0 \\ \mathbf{r}_F^0 \end{Bmatrix} \quad (21)$$

where $\mathbf{F}^0{}_{BB}(x)$, $\mathbf{F}^0{}_{BF}(x)$, $\mathbf{F}^F{}_B(x)$, and $\mathbf{F}^0{}_{FF}(x)$ are the following flexibility terms:

$$\begin{aligned}
\mathbf{F}_{BB}^0(x) &= \int_L \left(\mathbf{N}_{BB}^T(x)\mathbf{f}_B^0(x)\mathbf{N}_{BB}(x) + \mathbf{N}_{FB}^T(x)\mathbf{f}_F^0(x)\mathbf{N}_{FB}(x) \right) dx \\
\mathbf{F}_{BF}^0(x) &= \int_L \left(\mathbf{N}_{BB}^T(x)\mathbf{f}_B^0(x)\mathbf{N}_{BF}(x) + \mathbf{N}_{FB}^T(x)\mathbf{f}_F^0(x)\mathbf{N}_{FF}(x) \right) dx \\
\mathbf{F}_{FB}^0(x) &= \mathbf{F}_{BF}^{0^T}(x) \\
\mathbf{F}_{FF}^0(x) &= \int_L \left(\mathbf{N}_{BF}^T(x)\mathbf{f}_B^0(x)\mathbf{N}_{BF}(x) + \mathbf{N}_{FF}^T(x)\mathbf{f}_F^0(x)\mathbf{N}_{FF}(x) \right) dx
\end{aligned} \quad (22)$$

The element displacement $\mathbf{r}^0$ and foundation displacement $\mathbf{r}^0{}_F$ vectors are compatible with the beam-section deformation $\mathbf{d}^0{}_B(x)$ and foundation deformation $\mathbf{d}^0{}_F(x)$ vectors via the following integral expression as:

$$\begin{aligned}
\mathbf{r}^0(x) &= \int_L \left(\mathbf{N}_{BB}^T(x)\mathbf{d}_B^0(x) + \mathbf{N}_{FB}^T(x)\mathbf{d}_F^0(x) \right) dx \\
\mathbf{r}_F^0(x) &= -\int_L \left(\mathbf{N}_{BF}^T(x)\mathbf{d}_B^0(x) + \mathbf{N}_{FF}^T(x)\mathbf{d}_F^0(x) \right) dx
\end{aligned} \quad (23)$$

It is interesting to observe from the terms on the right-hand side of Eq. (21) that $\mathbf{U}-\mathbf{r}^0$ defines the element nodal displacement residuals associated with the element flexibility equation while $\boldsymbol{r}^0{}_F$ represents the known foundation displacements at selected reference points similar to a prescribed support condition in the method of consistent deformations. With the known foundation displacements $\mathbf{r}_F{}^0$, the reference foundation force vector $\Delta\mathbf{P}_F$ serving as the redundant-force unknowns can be eliminated using the second equation in Eq. (21).

$$\Delta\mathbf{P}_F = -\left(\mathbf{F}_{FF}^0\right)^{-1}\left(\mathbf{F}_{FB}^0\Delta\mathbf{P} + \mathbf{r}_F^0\right) \quad (24)$$

Substituting Eq. (24) into the first relation of Eq. (21) results in the condensed matrix compatibility equation as:

$$\mathbf{F}^0\Delta\mathbf{P} = \mathbf{U} - \left(\mathbf{U}_B^0 + \mathbf{U}_F^0\right) \quad (25)$$

where $\mathbf{F}^0 = \mathbf{F}_{BB}^0 - \mathbf{F}_{BF}^0\left(\mathbf{F}_{FF}^0\right)^{-1}\mathbf{F}_{FB}^0$ represents the element flexibility matrix; and $\mathbf{U}^0{}_B$ and $\mathbf{U}^0{}_F$ are the nodal displacement vectors compatible with the beam-section deformation $\mathbf{d}^0{}_B(x)$ and foundation deformation $\mathbf{d}^0{}_F(x)$ vectors, respectively and are defined as:

$$\begin{aligned}
\mathbf{U}_B^0 &= \int_L \left(\mathbf{N}_{BB}^T(x) - \mathbf{F}_{BF}^0\left(\mathbf{F}_{FF}^0\right)^{-1}\mathbf{N}_{BF}^T(x) \right)\mathbf{d}_B^0(x)\,dx \\
\mathbf{U}_F^0 &= \int_L \left(\mathbf{N}_{FB}^T(x) - \mathbf{F}_{BF}^0\left(\mathbf{F}_{FF}^0\right)^{-1}\mathbf{N}_{FF}^T(x) \right)\mathbf{d}_F^0(x)\,dx
\end{aligned} \quad (26)$$

It is worth pointing out that the term $\mathbf{U} - \left(\mathbf{U}_B^0 + \mathbf{U}_F^0\right)$ on the right-hand side of Eq. (25) defines the element nodal displacement residual vector and is associated with the integral statement of the beam-section and foundation compatibility conditions (Eqs. (11) and (13)). This residual vector becomes vanishing once the element compatible configuration is obtained during the incremental-iterative solution process.

In the present study, the general-purpose finite element platform FEAP (Taylor 2000) is employed to host the proposed beam-foundation element. The platform architect of FEAP is constructed within the framework of stiffness-based finite element formulation, thus rendering FEAP natural to the stiffness-based finite element model. Therefore, a special procedure for the element state determination is required for the proposed beam-foundation element formulated within the framework of flexibility-based finite element model. Fortunately, the state-of-the art procedure for implementing the flexibility-based finite element model into the stiffness-based computational platform was proposed by Spacone *et al.* (1996b) and Limkatanyu and Spacone (2002b). This procedure is adopted in the present work and is briefly discussed herein.

For a given current nodal displacement increment, the current nodal force increment is computed using the initial (last iterative step) element stiffness matrix and is used to update the nodal force vector. Then, the current section force increment associated with the current nodal force increment is computed using the force shape functions and the section force vector is updated accordingly. Next, the current section deformation increment associated with the current section force increment is computed using the initial (last iterative step) section flexibility matrix and the section

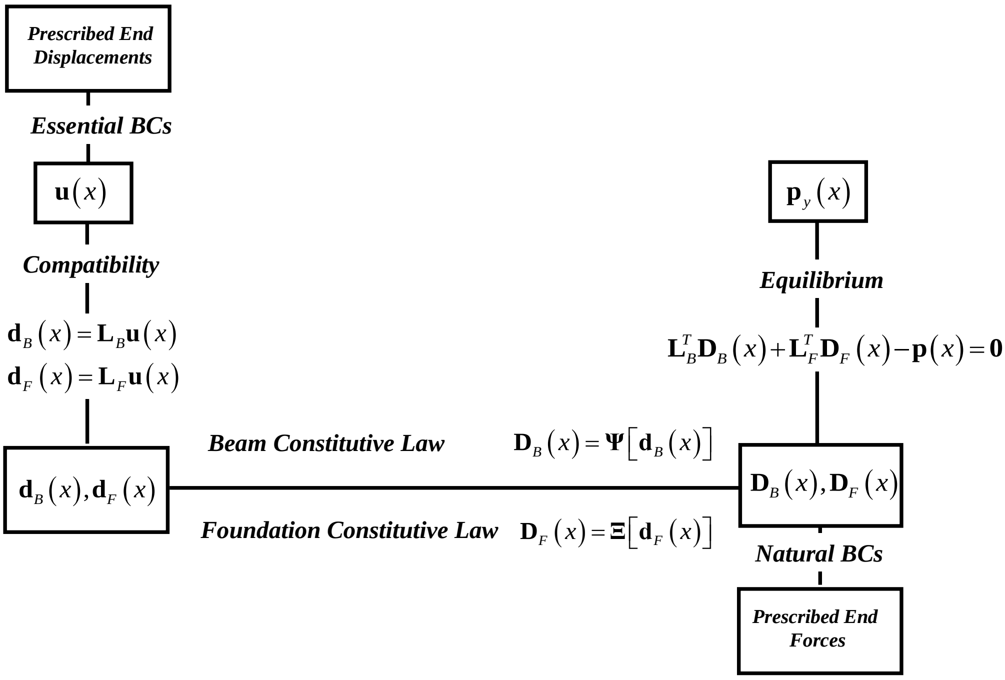

Fig. 3 Tonti's diagram for beam element on Winkler-Pasternak foundation: governing differential equations (Tonti 1976)

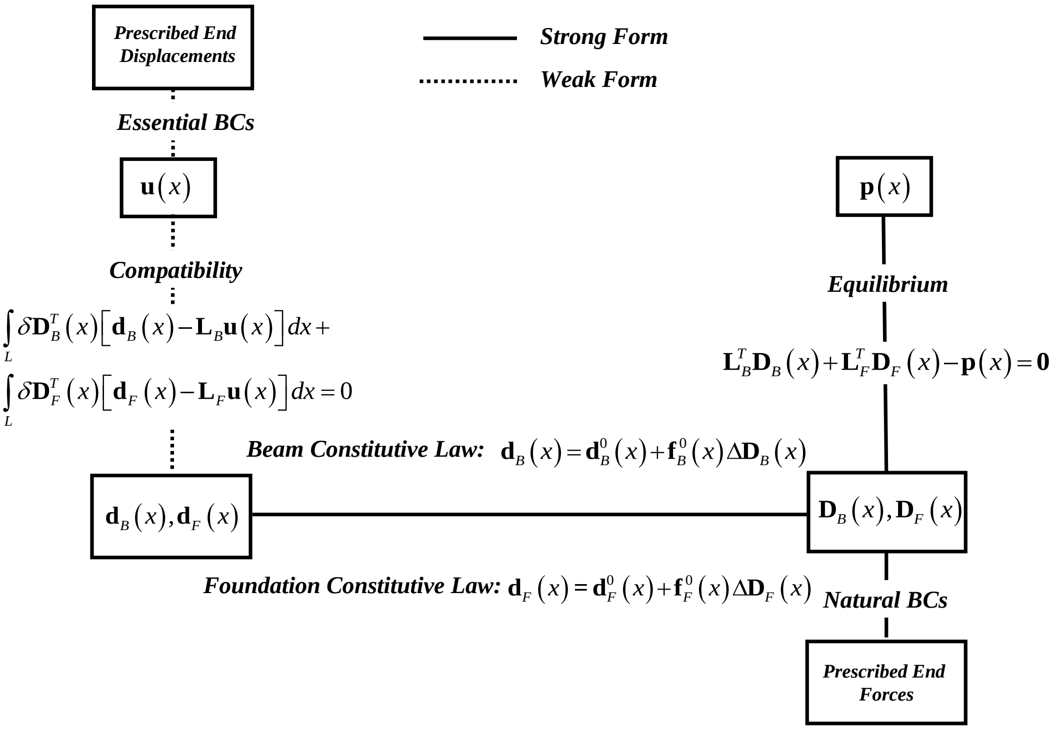

Fig. 4 Tonti's diagram for force-based beam element on Winkler-Pasternak foundation

deformation vector is updated accordingly. With the current (updated) section deformation vector, the associated section force vector and the associated section stiffness (flexibility) matrix can be obtained via the section constitutive relations. Generally, the current section force vector obtained from the section constitutive relations is not in equilibrium with the current nodal force vector, thus resulting in the unbalanced section force vector and the associated residual section deformation vector. The residual nodal displacement vector is computed from the residual section deformation vector using the integral expression of element compatibility. Finally, the unbalanced nodal force vector is computed from the residual nodal displacement vector and is passed from the element level to the structural level during the incremental-iterative solution process. More details on the above-discussed element state determination procedure can be found in Spacone *et al.* (1996b) and Limkatanyu and Spacone (2002b).

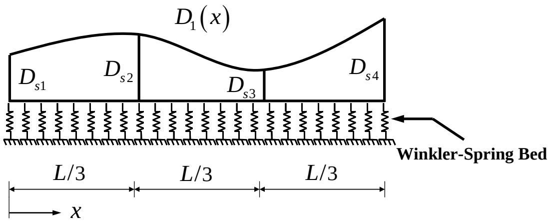

(a) Winkler-foundation interactive force

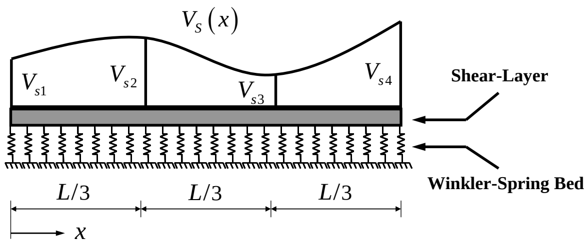

(b) Shear-layer section shear force

Fig. 5 Cubic foundation-force distributions along the element length

It is worthy to point out that the element stiffness matrix **K** can simply be obtained by inverting the element flexibility matrix **F** due to the presence of the underlying foundation. Therefore, the transformation between the complete and basic systems as required in a typical flexibility-based frame model is not necessary for the present problem.

3.2 Derivation of equilibrated force shape functions

Unlike in the case of an internally statically determinate beam, the internal force distribution of an internally statically indeterminate beam cannot be obtained solely from equilibrium consideration.Several researchers (Salari *et al.* 1998, Limkatanyu and Spacone 2002a, 2006) have attempted to formulate the flexibility-based finite beam elements to model these internally statically indeterminate beams by assuming certain internal force distribution, thus resulting in the internally statically determinate beams. In the present work, this assumed internal-force concept is adopted and extended to the flexibility-based finite element formulation of Winkler-Pasternak based beam foundation systems.

As indicated in Eq. (5), the problem of Winkler-Pasternak based beam-foundation systems is internally statically indeterminate. Thus, considering solely equilibrium condition is insufficient to determine three internal force fields, namely: beam-section bending $M_B(x)$, Winkler-foundation interactive force $D_1(x)$, and shear-layer section shear force $V_s(x)$. To render the Winkler-Pasternak based beam-foundation system internally statically determinate, Winkler-foundation interactive force $D_1(x)$, and shear-layer section shear force $V_s(x)$ are selected as redundant forces and their distributions are to be assumed. In the proposed beam-foundation model, the distributions of Winkler-foundation interactive force $D_1(x)$ and shear-layer section shear force $V_s(x)$ is represented by a third-order polynomial function. The degree of indeterminacy, however, is still infinite due to the continuous nature of the foundation-force distributions. This difficulty can be overcome by defining the foundation-force distributions in terms of a finite number of foundation-force distributions at selected reference points. Therefore, as shown in Fig. 5(a) and 5(b), Winkler-foundation interactive force $D_1(x)$ and shear-layer section shear force $V_s(x)$ are related to foundation forces at reference points in the following fashion:

$$D_1(x) = \left[\Phi_{s1}(x) \quad \Phi_{s2}(x) \quad \Phi_{s3}(x) \quad \Phi_{s4}(x)\right]\begin{Bmatrix} D_{s1} \\ D_{s2} \\ D_{s3} \\ D_{s4} \end{Bmatrix} \tag{27}$$

$$V_S(x) = \left[\Phi_{s1}(x) \quad \Phi_{s2}(x) \quad \Phi_{s3}(x) \quad \Phi_{s4}(x)\right]\begin{Bmatrix} V_{s1} \\ V_{s2} \\ V_{s3} \\ V_{s4} \end{Bmatrix} \tag{28}$$

where $\Phi_{s1}(x)$, $\Phi_{s2}(x)$, $\Phi_{s3}(x)$, and $\Phi_{s4}(x)$ are third-order polynomial shape functions and can define as:

$$\begin{aligned}&\Phi_{s1}(x) = 1 - \frac{11x}{2L} + \frac{9x^2}{L^2} - \frac{9x^3}{2L^3};\ \Phi_{s2}(x) = \frac{9x}{L} - \frac{45x^2}{2L^2} + \frac{27x^3}{2L^3};\\ &\Phi_{s3}(x) = -\frac{9x}{2L} + \frac{18x^2}{L^2} - \frac{27x^3}{2L^3};\ \Phi_{s4}(x) = \frac{x}{L} - \frac{9x^2}{2L^2} + \frac{9x^3}{2L^3}\end{aligned} \tag{29}$$

The Winkler-foundation interactive forces at reference points D_{s1}, D_{s2}, D_{s3}, and D_{s4} and the shear-layer section shear forces at reference points V_{s1}, V_{s2}, V_{s3}, and V_{s4} are not entirely independent since two of them can be expressed in terms of the remaining six reference forces and of the beam nodal forces after enforcing the external (global) equilibrium conditions of the beam component of the beam-foundation element (Fig. 6(a)).

Considering the moment equilibrium condition of the beam component (Fig. 6(b)) leads to the following expression:

$$P_2 + P_4 + \left(P_3 + V_{s4}\right)L - \int_L xD_2(x)dx = 0 \tag{30}$$

Employing Eqs. (27) and (28) and enforcing the equilibrium condition of Eq. (4), Eq. (30) becomes:

$$\begin{aligned}&P_2 + P_4 - \frac{L}{120}(L(2D_{s1} + 9D_{s2} + 36D_{s3} + 13D_{s4})\\ &-15(V_{s1} + 3(V_{s2} + V_{s3}) - 7V_{s4})) + L(P_3 + V_{s4}) = 0\end{aligned} \tag{31}$$

Considering the vertical equilibrium condition of the beam component (Fig. 6(b)) yields the following expression:

$$P_1 + P_3 - V_{s1} + V_{s4} - \int_L D_2(x)\,dx = 0 \tag{32}$$

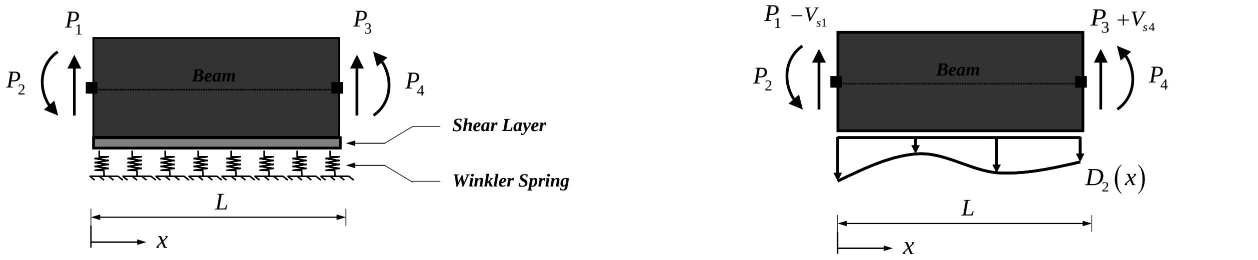

(a) Beam-foundation element (b) Beam component with foundation-interactive force

Fig. 6 Proposed beam element on Winkler-Pasternak foundation

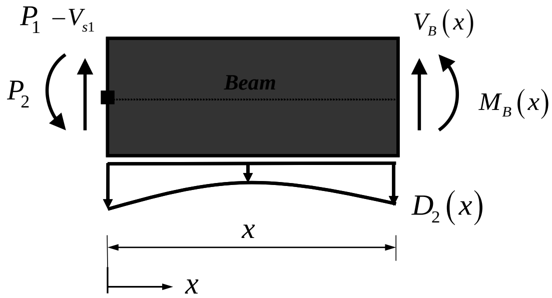

Fig. 7 Cut beam segment

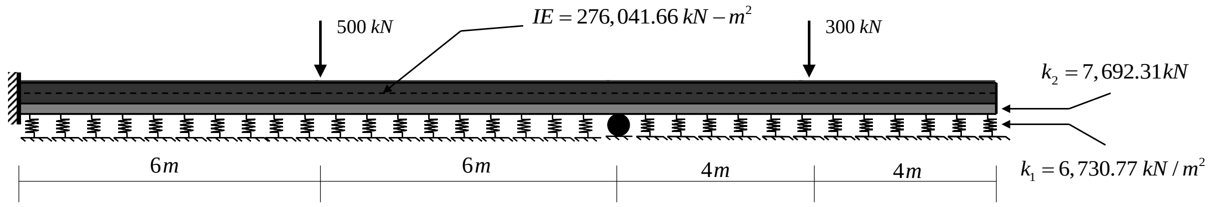

Fig. 8 Example I: continuous beam on Winkler-Pasternak foundation under in-span concentrated loads (Aslami and Akimov 2016)

Using Eqs. (27) and (28) and enforcing the equilibrium condition of Eq. (4), Eq. (32) becomes:

$$8P_1 + 8P_3 - L(D_{s1} + 3(D_{s2} + D_{s3}) + D_{s4}) = 0 \tag{33}$$

Based on Eqs. (31) and (33), two reference foundation forces D_{s4} and V_{s4} are related to remaining six reference foundation forces and element nodal forces as:

$$D_{s4} = \frac{8P_1 + 8P_3 - L(D_{s1} + 3(D_{s2} + D_{s3}))}{L} \tag{34}$$

$$V_{s4} = \frac{1}{15L}\begin{bmatrix} -120P_2 - 120P_4 + L^2(2D_{s1} + 9D_{s2} + 36D_{s3} + 13D_{s4}) \\ -15L(8P_3 + V_{s1} + 3(V_{s2} + V_{s3})) \end{bmatrix} \tag{35}$$

Substituting Eqs. (34) and (35) into Eqs. (27) and (28), the foundation-section force vector $\mathbf{D}_F(x)$ can be expressed as:

$$\mathbf{D}_F(x) = \mathbf{N}_{FB}(x)\mathbf{P} + \mathbf{N}_{FF}(x)\mathbf{P}_F \tag{36}$$

where $\mathbf{P} = \{P_1 \quad P_2 \quad P_3 \quad P_4\}^T$ is an array containing the element nodal forces; and $\mathbf{P}_F = \{D_{s1}\ D_{s2}\ D_{s3}\ V_{s1}\ V_{s2}\ V_{s3}\}^T$ is an array collecting the reference foundation-interactive forces. The expression for each foundation-force shape function in matrices $\mathbf{N}_{FB}(x)$ and $\mathbf{N}_{FF}(x)$ is given in Appendix.

Considering the moment equilibrium of Fig. 7, the sectional moment $M_B(x)$ becomes:

$$M_B(x) = \int_x x D_2(x)\,dx + (P_1 - V_{s1})x - P_2 - x\int_x D_2(x)\,dx \tag{37}$$

Employing Eqs. (27) and (28) and enforcing the equilibrium condition of Eq. (4), Eq. (37) can be written in the matrix form as:

$$\mathbf{D}_B(x) = \mathbf{N}_{BB}(x)\mathbf{P} + \mathbf{N}_{BF}(x)\mathbf{P}_F \tag{38}$$

The expression for each beam-section force shape function in matrices $\mathbf{N}_{BB}(x)$ and $\mathbf{N}_{BF}(x)$ is given in Appendix.

4. Numerical validation

The validity and effectiveness of the proposed beam-foundation model are assessed through three numerical simulations. The first simulations focus on elastic beam-foundation systems while the last simulation emphasizes on an inelastic beam-foundation system.

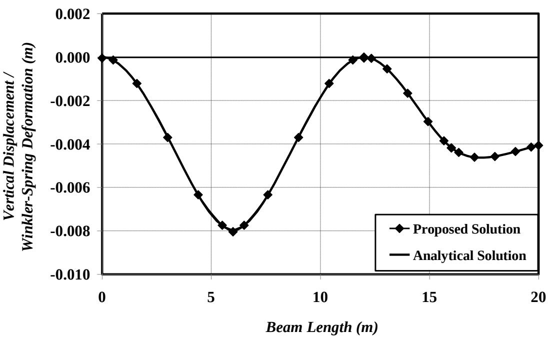

(a) Vertical displacement diagram

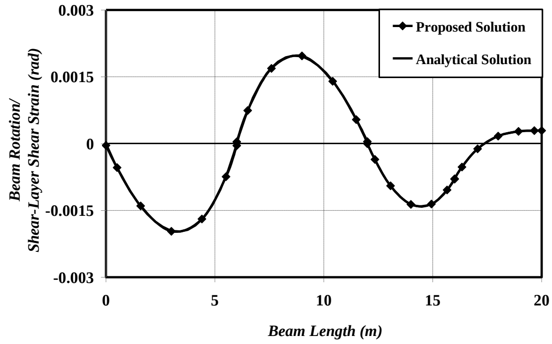

(b) Beam rotation diagram

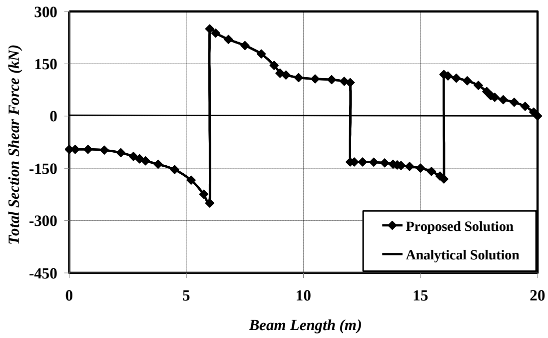

(c) Total section shear force diagram

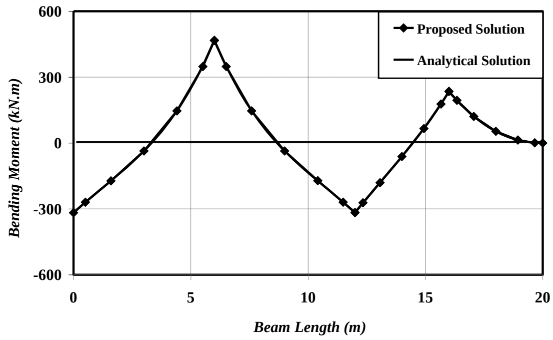

(d) Bending moment diagram

Fig. 9 Beam responses of Simulation I

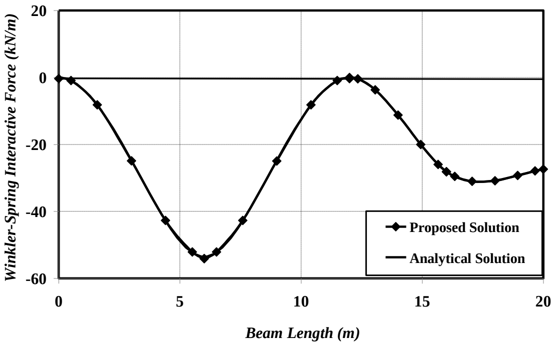

(a) Winkler-spring interactive force diagram

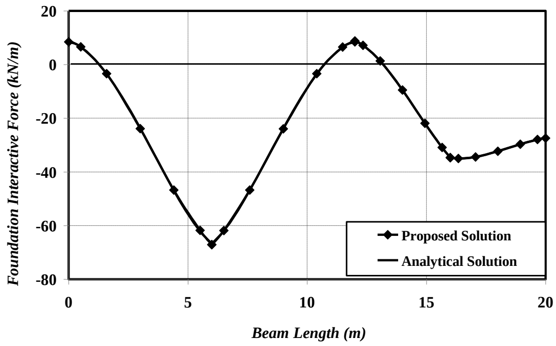

(b) Foundation interactive force diagram

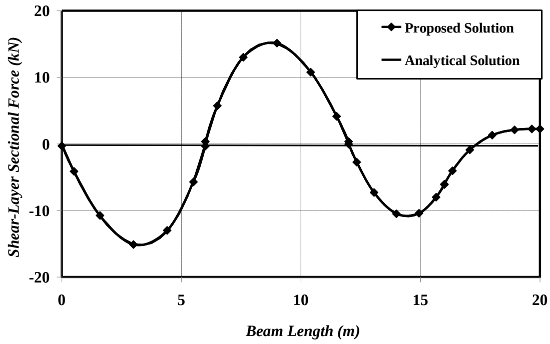

(c) Shear-layer sectional force diagram

Fig. 10 Diagrams for internal foundation forces of Simulation I

4.1 Simulation I

Fig. 8 shows the beam-foundation system modified from by Aslami and Akimov (2016). All system geometric and mechanical properties shown in Fig. 8 are provided by Aslami and Akimov (2016). The foundation stiffness parameters (k_1 and k_2) are computed using the Vlasov model(Vlasov and Leontiev 1966). To represent the beam-foundation system of Fig. 8, each beam span is discretized by only one proposed element. Therefore, the whole system

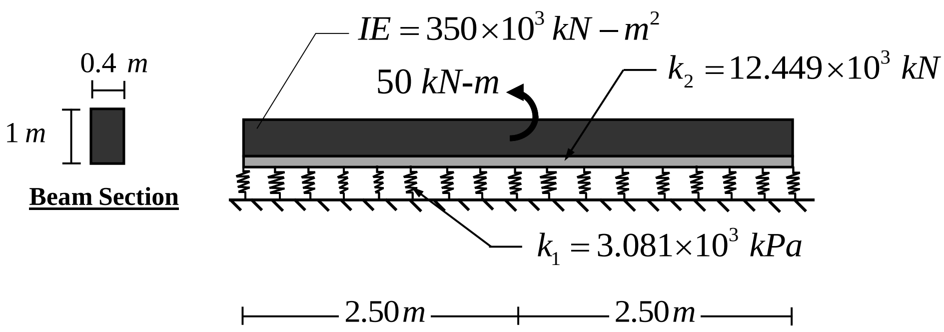

Fig. 11 Example II: prismatic beam on Winkler-Pasternak foundation under a midspan moment (Mullapudi and Ayoub 2010, Sapountzakis and Kampitsis 2013)

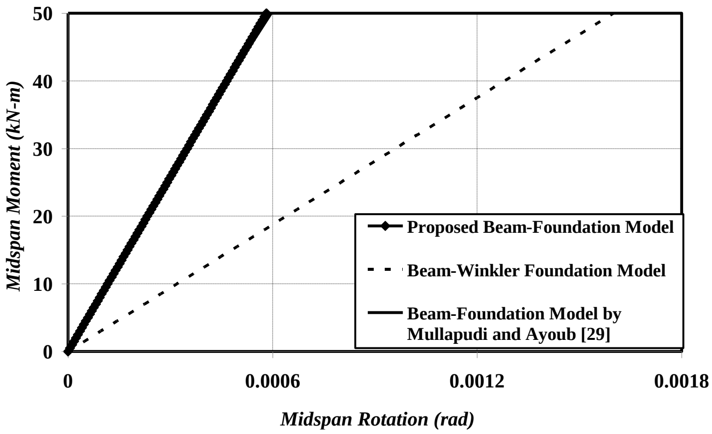

Fig. 12 Moment-rotation responses for example II

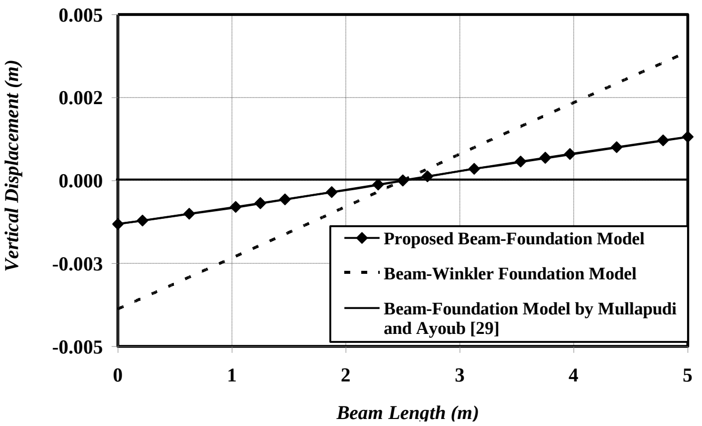

Fig. 13 Vertical displacement profiles for example II

is discretized by four proposed beam-foundation elements, hence resulting in seven nodal unknowns.

Fig. 9 shows the obtained beam-section response diagrams while Fig. 10 plots the computed foundation force diagrams. For comparison, the analytical responses based on the solution by Gülkan and Alemdar (1999) are also superimposed on the same diagrams. The validity and effectiveness of the proposed model are clearly noticed in Figs. 9 and 10. It is worth pointing out that this beam-foundation system is also analyzed by the stiffness-based beam-foundation model with cubic displacement shape functions proposed by Zhaohua and Cook (1983). To gain satisfactory nodal-displacement values (at points *B* and *D*), two stiffness-based elements per beam span are needed, thus resulting in fifteen nodal unknowns. Moreover, four stiffness-based elements per beam span (thirty one nodal unknowns) are required to satisfactorily represent the beam-section and foundation force variations along the length.

4.2 Simulation II

A free-free Winkler-Pasternak based beam-foundation system is exerted by a concentrated moment of 50 kN-m at its mid-span as shown in Fig. 11. Several researchers (Shirima and Giger 1992, Mullapudi and Ayoub 2010, Sapountzakis and Kampitsis 2013) have employed this beam-foundation problem to reference their proposed

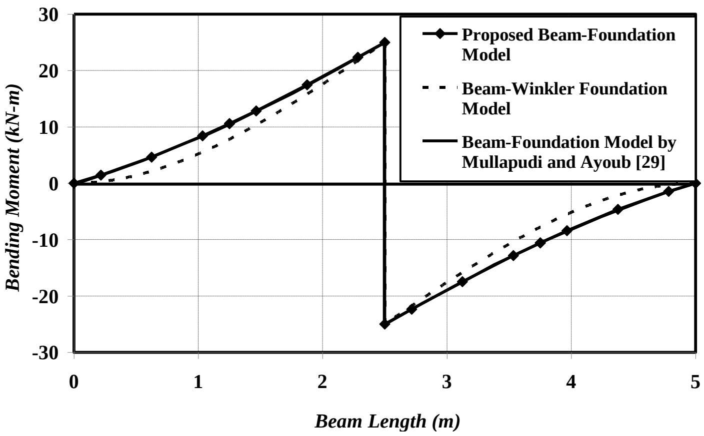

Fig. 14 Bending-moment diagrams for example II

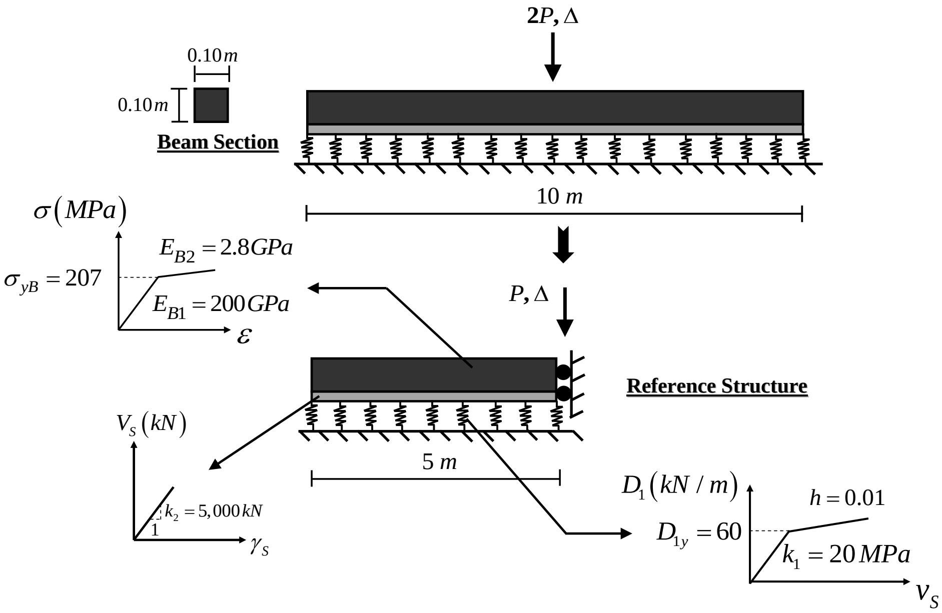

Fig. 15 Example III: inelastic Winkler-Pasternak beam-foundation system under a midspan load (Limkatanyu *et al.* 2015)

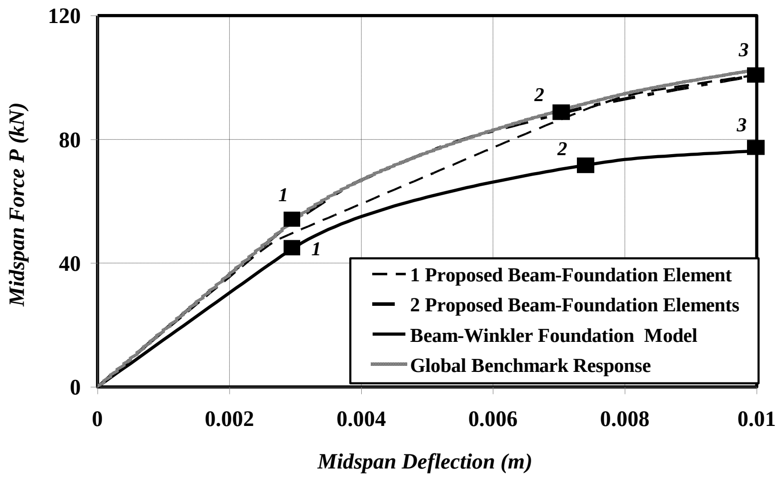

Fig. 16 Global convergence studies of the proposed beam-foundation model

models. Geometric properties of the timber beam follow those given by Mullapudi and Ayoub (2010). The beam is 5-*m* long and has a rectangular cross-section of 0.4 x 1.0 m^2. The elastic modulus of timber is E_t= 10.5 GPa. Thus, the flexural rigidity is IE= 350 x 10^3 kN-m^2. The underlying soil is sandy clay with an elastic modulus E_s= 45.5 MPa and

Poisson ration v_s= 0.25. The foundation stiffness parameters (k_1 and k_2) associated with these soil elastic properties are k_1= 3.081 x 10^3 kPa and k_2= 12.449 x 10^3 kN as given in Mullapudi and Ayoub (2010) using the Vlasov model (Vlasov and Leontiev 1966). The beam-foundation system of Fig. 11 is represented by two proposed beam-foundation elements (one for each half). This beam-foundation system is also analyzed using the Winkler-based beam element (Limkatanyu *et al.* 2013) to investigate the influences of employed foundation models on system behaviors.

Fig. 12 shows the moment-rotation responses at the beam midspan obtained from different beam-foundation models. On the same diagram, the response obtained with four beam-Winkler-Pasternak mixed elements of Mullapudi and Ayoub (2010) is also superimposed for the verification of the beam-foundation element proposed herein. It is clear from Fig. 12 that two proposed beam-foundation elements result in the moment-rotation response as accurate as that obtained with four beam-Winkler-Pasternak mixed elements of Mullapudi and Ayoub (2010), thus confirming the validity and effectiveness of the proposed model. Furthermore, the response obtained with Winkler foundation model is much more flexible than that obtained with Winkler-Pasternak foundation model. The maximum midspan rotation obtained with Winkler foundation model is about 2.75 times larger than that obtained with Winkler-Pasternak foundation model. The enhanced rotational stiffness associated with Winkler-Pasternak foundation model is due to consideration of soil continuity within the underlying soil medium.

Fig. 13 presents the beam displacement profiles obtained with different beam-foundation models. These displacement profiles are associated with the concentrated moment of 50 kN-m at its midspan. The proposed model and the beam-Winkler-Pasternak mixed model proposed by Mullapudi and Ayoub (2010) result in the same beam displacement profile. As expected, the Winkler-based beam model yields larger vertical displacements at beam ends. The end displacement obtained with the Winkler-based beam model is about 2.94 times larger than that obtained with the proposed beam-Winkler-Pasternak model thanks to the coupling between the Winkler foundation springs via the shear-layer foundation component.

Fig. 14 shows the bending moment diagrams obtained with different beam-foundation models. These bending moment diagrams are corresponding to the midspan concentrated moment of 50 kN-m. The proposed model and the beam-Winkler-Pasternak mixed model proposed by Mullapudi and Ayoub (2010) yields the same bending moment diagram. It is observed that the bending moment profile is slightly under-predicted when the soil continuity within the underlying soil medium is not taken into account as obtained with the Winkler-based beam model.

4.3 Simulation III

Fig. 15 shows a free-free Winkler-Pasternak based beam-foundation system under the exertion of a midspan point load. Limkatanyu *et al.* (2015) also analyzed this beam-foundation system using the improved stiffness-based beam-Winkler-Pasternak foundation element. The finite-element discretization is necessary only for half of the system thanks to the system symmetry. The properties of the beam geometry and beam material are given by Mullapudi and Ayoub (2010). The fiber-section model is used to represent the inelastic beam-section response. A section discretization of twenty fibers (layers) is employed to represent the beam sectional response. The bilinear elastic-plastic model is employed to represent each beam-fiber response with a first stiffness E_{B1}= 200 GPa, a yield strength σ_{yB}= 207 MPa, and a second stiffness E_{B2}= 2.8 GPa. The Winkle spring bed is characterized by a bilinear elastic-plastic model while the Pasternak shear layer is represented by a linearly elastic model. For the Winkler spring bed, an initial modulus k_1 is 20 MPa; a yielding force D_{1y} is 60 kN/m; and a strain-hardening ratio is 0.01. For the elastic Pasternak shear layer, its stiffness k_2 is 5,000 kN. These mechanical properties of the foundation model are provided by Sapountzakis and Kampitsis (2013).

Fig. 16 examines the required numbers of elements to yield the converged global response (midspan load-deflection relation) for the proposed Winkler-Pasternak beam-foundation model and investigates the inelastic behavior of the system using different foundation models. This beam-foundation system is also analyzed by two stiffness-based beam models (Mullapudi and Ayoub 2010, Limkatanyu *et al.* 2015) to compare their validity and effectiveness with the Winkler-Pasternak based beam-foundation model proposed herein. A finite-element mesh of 32 stiffness-based beam elements with cubic shape functions is employed to obtain the so-called "*reference*" global response. The response curves obtained with the proposed model indicate that a mesh containing 2 elements can resemble the reference global response. It is interesting to observe that an increase in the number of proposed elements leads to stiffer responses (convergence from below). This convergence characteristic is associated with the flexibility-based finite element formulation (the virtual force principle) and is in opposition to the stiffness-based finite element formulation (the virtual displacement principle) in which an increase in the number of elements results in a more flexible response (convergence from above). The convergence studies on the performance of two aforementioned stiffness-based models had been conducted and indicated that 8 stiffness-based beam elements with cubic shape functions and 2 stiffness-based beam elements with improved shape functions were required to reproduce the reference global response, hence showing the validity and effectiveness of the proposed flexibility-based model. Even though the stiffness-based beam-foundation model proposed by Limkatanyu *et al.* (2015) is as accurate as the proposed flexibility-based beam-foundation model for the global response, the advantage of the flexibility-based model proposed herein over the stiffness-based model in representing the local response is to be pointed out subsequently. To show the influences of employed foundation models, the response obtained with the Winkler-based beam-foundation model proposed by Limkatanyu *et al.* (2013) is also added into Fig. 16. There are three loading points marked on the response curves in Fig. 16; Point *1* at which the Winkler-spring bed first reaches its yielding

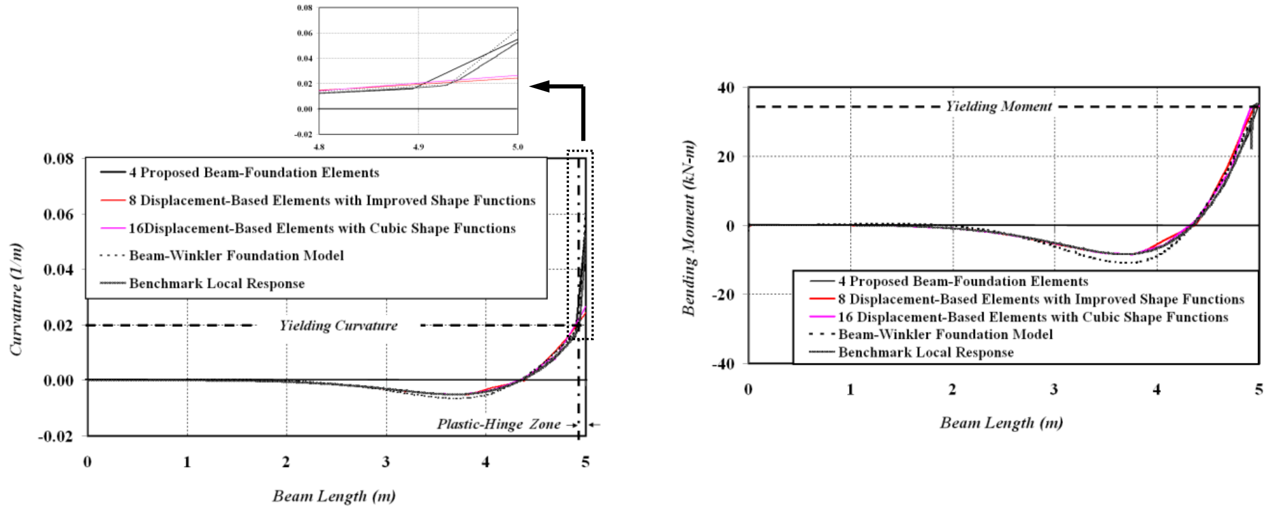

(a) Curvature diagram (b) Moment diagram

Fig. 17 Moment and curvature distributions along the beam for midspan displacement δ = 0.01 m

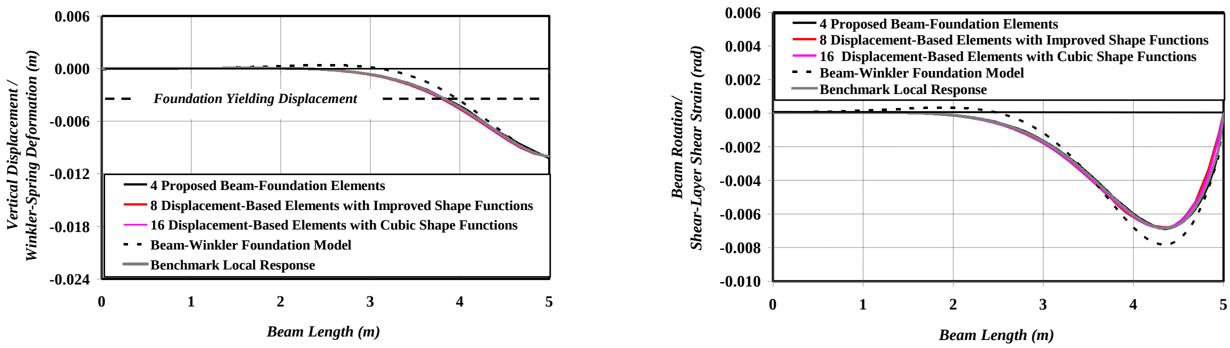

(a) Vertical displacement diagram (b) Beam rotation diagram

Fig. 18 Vertical displacement and beam rotation distributions along the beam for midspan displacement δ = 0.01 m

strength; Point 2 at which the plastic hinge first forms at the beam midspan; and Point 3 at which the midspan deflection of Δ = 0.01 m is attained. Fig. 16 shows that an initial stiffness of the Winkler-Pasternak based beam-foundation system is approximately 1.20 times higher than that of the Winkler based beam-foundation system (Point *1*). The Winkler-Pasternak foundation model can lead to an increase in the midspan load causing the midspan plastic-hinge formation (Point *2*) about 25 percent when compared to the Winkler foundation model. The midspan load associated with Point *3* also increases approximately 34 percent when the Winkler foundation is replaced by the Winkler-Pasternak foundation model. Associated with the added shear-layer foundation component to account for soil continuity, the stiffer and stronger load-deflection response of the Winkler-Pasternak beam-foundation system is obtained.

The local-response convergence studies of the beam-foundation system reveal that four proposed elements can resemble the reference local responses as shown in Figs. 17-19. It is noted that a finite-element mesh of 64 stiffness-based beam elements with cubic shape functions is employed to obtain the reference local responses. The local-response convergence studies of two aforementioned stiffness-based models had also been performed and indicated that 16 stiffness-based beam elements with cubic shape functions and 8 stiffness-based beam elements with improved shape functions were required to reproduce the reference local responses, thus showing the validity and effectiveness of the proposed flexibility-based beam-foundation element.

Fig. 17 shows the bending-curvature and bending-moment distributions at integration points along the beam length under an imposed midspan deflection of Δ = 0.01 m (Point *3*). In general, a relatively coarse mesh of 4 proposed beam-foundation elements can reproduce the reference beam-section local responses. Although 16 stiffness-based elements of Mullapudi and Ayoub (2010) and 8 stiffness-based elements of Limkatanyu *et al.* (2015) are able to resemble the overall distributions of the beam section responses, they both underestimate the maximum curvature by factors of 1.98 and 2.29, respectively as shown in the inset of Fig. 17(a). However, the proposed flexibility-based model is able to accurately predict the maximum curvature as shown in the inset of Fig. 17(a) due to the merit of force shape functions, thus confirming the superiority of the proposed model in representing the local responses. This feature could be essential especially when the beam-section

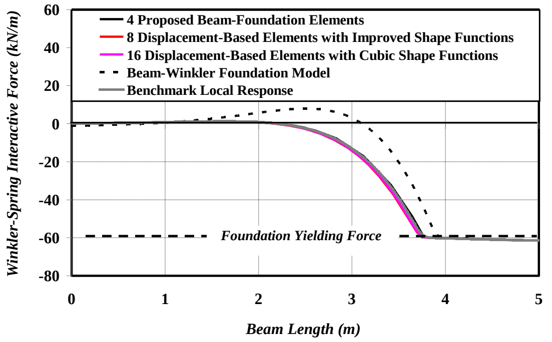

(a) Winkler-spring interactive force diagram

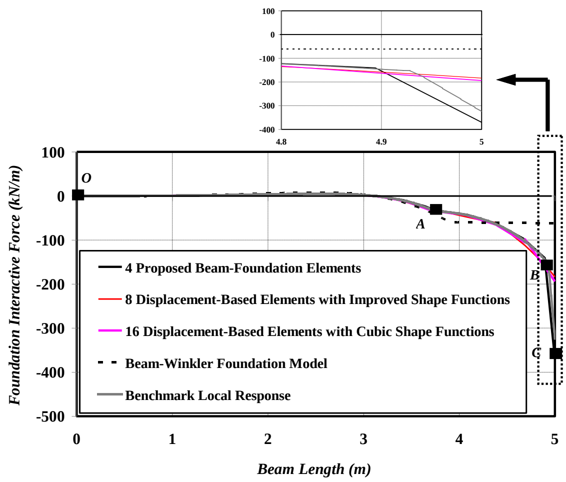

(b) Foundation interactive force diagram

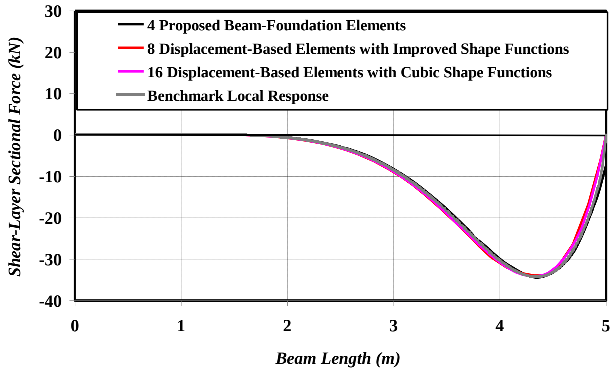

(c) Shear-layer sectional force diagram

Fig. 19 Internal foundation force distributions along the beam for midspan displacement δ = 0.01 m

curvature ductility becomes a critical consideration in design and assessment of the beam-foundation system under seismic loadings (ICC 2012). Unlike those obtained with stiffness-based models, the bending-moment distribution obtained with the proposed model shows no sudden drop in the plastic-hinge region. This sudden drop in the moment distribution was also detected in Limkatanyu and Spacone (2002a) and could be remedied by employing the flexibility-based beam formulation (Limkatanyu and Spacone 2006) or mixed beam formulation (Mullapudi and Ayoub 2010). Furthermore, Fig. 17(b) shows that the employed foundation model affects the maximum values of negative moment (concave) and bending curvature. The Winkler-Pasternak foundation model results in a 22.9 % decrease in the maximum negative moment and a 15.9 % decrease in the maximum bending curvature. These reductions are associated with the merit of the stiffer and stronger foundation model employed in mitigating the beam bending response.

Fig. 18 shows the beam vertical displacement and beam rotation distributions at integration points along the beam length under an imposed midspan deflection of Δ = 0.01 m (Point 3). Following the compatibility hypothesis of the adopted Winkler-Pasternak foundation model, Fig. 18 also shows the Winkler-spring deformation and shear-layer shear strain distributions. Clearly, a relative coarse mesh of 4 proposed elements can produce the reference beam vertical displacement and beam rotation distributions. To present the computational effectiveness of the proposed model, the beam-section displacement distributions obtained with two stiffness-based models are also superimposed in Fig. 18. Furthermore, the beam-section displacement distribution obtained with the Winkler foundation model is presented in Fig. 18. The beam deflection profiles of Fig. 18(a) obtained from both foundation models indicates that in this numerical simulation, the beam-foundation system can be considered as an infinitely long beam-foundation system. Associated with added restraint by the shear-layer foundation component, the Winkler-Pasternak beam-foundation system sinks into the ground (negative displacement), while a certain part of the Winkler beam-foundation system (from 1.25 to 3.1 m) lifts off the ground (positive displacement). The shear-layer foundation component plays an enhancing role in reducing the beam rotation as shown in Fig. 18(b), thus leading to a 12.8 % decrease in the maximum beam rotation.

Fig. 19 plots the foundation force diagrams under an imposed midspan deflection of Δ= 0.01 m (Point *3*). Obviously, a relative coarse mesh consisting of 4 proposed elements is sufficient in resembling the reference foundation-force distributions. Comparisons between the foundation-force distributions associated with the proposed flexibility-based model and two stiffness-based models shows the computational efficiency of the proposed flexibility-based model. The foundation-force distributions obtained with the Winkler-based beam model are also superimposed into Fig. 19. Comparisons between the Winkler-spring interactive forces associated with two foundation models as shown in Fig. 19(a) indicate that the yielding region of the Winkler-foundation spring associated with the Winkler-Pasternak foundation model seems to spread out along a larger portion of the beam than that associated with the Winkler foundation model. This observation is due to the merit of the interaction between the Winkler-foundation springs. Fig. 19(b) shows that the shear-layer foundation component drastically alters distribution nature of the foundation interactive forces acting at the bottom face of the beam. There are three regions in the Winkler-Pasternak foundation force distribution, namely: 0-1, 1-2, and 2-3. Along region 0-1, all foundation components are in the elastic range; along region *1-2*, the yielding limit of the Winkler-foundation spring is reached while further increase of the foundation interactive force is associated with the added shear-layer foundation component; and along region *2-3* (plastic-hinge zone), the foundation interactive force drastically rises associated with the rapid increase in beam curvature as presented in Fig. 17(a). The maximum foundation interactive force shown in the inset of Fig. 19(b) can be predicted well by the proposed but is drastically underestimated by two stiffness-based models. This superiority of the proposed model is associated with its capability to represent well the maximum bending curvature as shown in Fig. 17(a). Due to linearly elastic response of the shear-layer foundation component, the shear-layer sectional force diagram of Fig. 19(c) simply resembles the shape of the shear-layer shear strain diagram of Fig. 18(b).

5. Conclusions

A novel flexibility-based beam-foundation model for inelastic analyses of beams on deformable foundation is proposed herein. To represent the underlying foundation medium, the Winkler-Pasternak foundation model is adopted. In this foundation model, the continuous nature of the underlying foundation is taken into account by laying an incompressible shear layer on the top ends of the Winkler-foundation spring bed. The principle of virtual forces forms the core of the proposed model. The internal force fields are related to the element force degrees of freedom through equilibrated force shape functions. To present the general procedure of both strong and weak forms of the problem, Tonti's diagrams are used. Three numerical simulations are employed to assess validity and to show effectiveness of the proposed model. An elastic continuous beam-foundation system under in-span concentrated forces is investigated in the first simulation. The simulation results confirm the model ability to represent analytical responses at both global and local levels. The model accuracy allows each beam span to be discretized only by a single proposed element, thus minimizing the computational cost. An elastic free-free beam-foundation system under a midspan moment is studied in the second simulation. The simulation results show the superiority of the proposed model over the mixed model proposed by Mullapudi and Ayoub (2010). When compared to the Winkler foundation model, the Winkler-Pasternak foundation model results in a stiffer beam-foundation system due to the added shear-layer foundation component to account for soil continuity. An inelastic free-free beam-foundation system under a midspan load is investigated in the third simulation. Based on global and local convergence studies, the superiority of the proposed model over stiffness-based models previously proposed in the literature (Mullapudi and Ayoub 2010, Limkatanyu *et al.* 2015) is confirmed. The added shear-layer foundation component associated with the Winkler-Pasternak foundation model results in a stiffer and stronger beam-foundation system and plays an essential role in characterizing the foundation-interactive force distribution.

Acknowledgments

The financial support of this work was provided by the Thailand Research Fund (TRF) under Grant RTA6280012 and by the National Research Foundation of Korea (NRF) grant funded by the Korea government (MSIT) (No.2019R1A2C1003007). Special thanks go to a senior lecturer Mr. Wiwat Sutiwipakorn for reviewing and correcting the English of this paper.

References

Aslami, M. and Akimov, P.A. (2016), "Analytical solution for beams with multipoint boundary conditions on two-parameter elastic foundations", *Arch. Civ. Mech. Eng.*, **16**(4), 668-677. https://doi.org/10.1016/j.acme.2016.04.005.

Bohlooly, M. and Fard, K.M. (2019), "Buckling and postbuckling of concentrically stiffened piezo-composite plates on elastic foundations", *J. Appl. Comput. Mech.*, **5**(1), 128-140. https://doi.org/10.22055/jacm.2018.25539.1277.

Civalek, O. and Ozturk, B. (2010), "Free vibration analysis of tapered beam-column with pinned ends embedded in Winkler-Pasternak elastic foundation", *Geomech. Eng.*, **2**(1), 45-56. https://doi.org/10.12989/gae.2010.2.1.045.

Demir, C., Mercan, K., Numanoglu, H.M. and Civalek, O. (2018), "Bending response of nanobeams resting on elastic foundation", *J. Appl. Comput. Mech.*, **4**(2), 105-114. https://doi.org/10.22055/jacm.2017.22594.1137.

Dutta, S.C. and Roy, R.A. (2002), "Critical review on idealization and modeling for interaction among soil-foundation-structure system", *Comput. Struct.*, **80**(20-21), 1579-1594. https://doi.org/10.1016/S0045-7949(02)00115-3.

Ebrahimi, F. and Barati, M.R. (2017), "Modeling of smart magnetically affected flexoelectric/piezoelectric nanostructures incorporating surface effects", *Nanomater. Nanotechnol.*, **7**(2), 1-11. https://doi.org/10.1177/1847980417713106.

Eisenberger, M. and Yankelevsky, D.Z. (1985), "Exact stiffness matrix for beams on elastic foundation", *Comput. Struct.*, **21**(6), 1355-1359. https://doi.org/10.1016/0045-7949(85)90189-0.

Feng, D.C., Wu, G. and Ning, C.L. (2019), "A regularized force-based Timoshenko fiber element including flexure-shear interaction for cyclic analysis of RC structures", *Int. J. Mech. Sci.*, **160**, 59-74. https://doi.org/10.1016/j.ijmecsci.2019.06.011.

Gangadean, D., Mcilroy, D.N., Faulkner, B.E. and Aston D.E. (2010), "Winkler boundary conditions for three-point bending tests on 1D nanomaterials", *Nanotechnol.*, **21**(22), 1-19. https://doi.org/10.1088/0957-4484/21/22/225704.
Ghosh, P., Rajesh, S. and Chand, J.S. (2017), "Linear and nonlinear elastic analysis of closely spaced strip foundations using Pasternak model", *Front. Struct. Civ. Eng.*, **11**(2), 228-243. https://doi.org/10.1007/s11709-016-0370-x.
Gülkan, P. and Alemdar, B.N. (1999), "Exact finite element for a beam on a two-parameter elastic foundation: A revisit", *Struct. Eng. Mech.*, **7**(3), 259-276. https://doi.org/10.12989/sem.1999.7.3.259.
He, X.G. and Kwan, A.K.H. (2001), "Modeling dowel action of reinforcement bars for finite element analysis of concrete structures", *Comput. Struct.*, **79**(6), 595-604. https://doi.org/10.1016/S0045-7949(00)00158-9.
Hetenyi, M. (1946), *Beams on Elastic Foundations*, University of Michigan Press, Ann Arbor, Michigan, U.S.A.
Horvath, J.S. and Colasanti, R.J. (2011), "Practical subgrade model for improved soil-structure interaction analysis: Model development", *Int. J. Geomech.*, **11**(1), 59-64. https://doi.org/10.1061/(ASCE)GM.1943-5622.0000070.
ICC (2012), International building code, International Code Council, Country Club Hills, Illinois, U.S.A.
Jafari, V., Abyaneh, M.A., Vahdani, S.H. and Rahimian M. (2009), "Improved displacement-field approximation for geometrical nonlinear flexibility-based planar curved element in state space", *Mech. Based Des. Struct. Mach.*, **37**(4), 475-502. https://doi.org/10.1080/15397730903164094.
Jamil, I. and Ahmad, I. (2019), "Bending moments in raft of a piled raft system using Winkler analysis", *Geomech. Eng.*, **18**(1), 41-48. https://doi.org/10.12989/gae.2019.18.1.041.
Kerr, A.D. (1964), "Elastic and viscoelastic foundation models", *J. Appl. Mech.*, **31**(4), 491-498. https://doi.org/10.1115/1.3629667.
Khemis, A., Chaouche, A.H., Athmani, A. and Tee, K.F. (2016), "Uncertainty effects of soil and structural properties on the buckling of flexible pipes shallowly buried in Winkler foundation", *Struct. Eng. Mech.*, **59**(4), 739-759. https://doi.org/10.12989/sem.2016.59.4.739.
Kim, S., Ceylan, H. and Gopalakrishnan, K. (2014), "Finite element modeling of environmental effects on rigid pavement deformation", *Front. Struct. Civ. Eng.*, **8**(2), 101-114. https://doi.org/10.1007/s11709-014-0254-x.
Kim, J.S., Kim, M.K. and Jung, S.D. (2015), "Two-dimensional numerical tunnel model using a Winkler-based beam element and its application into tunnel monitoring systems", *Cluster Comput.*, **18**(2), 707-719. https://doi.org/10.1007/s10586-014-0418-4.
Limkatanyu, S. and Spacone, E. (2002a), "Reinforced concrete frame element with bond interfaces. I: Displacement-based, force-based, and mixed formulations", *J. Struct. Eng.*, **128**(3), 346-355. https://doi.org/10.1061/(ASCE)0733-9445(2002)128:3(346).
Limkatanyu, S. and Spacone, E. (2002b), "Reinforced concrete frame element with bond interfaces. II: State determination and numerical validations", *J. Struct. Eng.*, **128**(3), 356-364. https://doi.org/10.1061/(ASCE)0733-9445(2002)128:3(356).
Limkatanyu, S. and Spacone, E. (2006), "Frame element with lateral deformable supports: Formulations and numerical validation", *Comput. Struct.*, **84**(13-14), 942-954. https://doi.org/10.1016/j.compstruc.2005.12.002.
Limkatanyu, S., Kwon, M., Prachasaree, W. and Chaiviriyawong, P. (2012a), "Contact interface fiber section element: Shallow foundation modeling", *Geomech. Eng.*, **4**(3), 173-190. https://doi.org/10.12989/gae.2012.4.3.173.
Limkatanyu, S., Kuntiyawichai, K., Spacone, E. and Kwon, M. (2012b), "Natural stiffness matrix for beams on Winkler foundation: Exact force-based derivation", *Struct. Eng. Mech.*, **42**(1), 39-53. https://doi.org/10.12989/sem.2012.42.1.039.
Limkatanyu, S., Kuntiyawichai, K., Spacone, E. and Kwon, M. (2013), "Nonlinear Winkler-based beam element with improved displacement shape functions", *KSCE J. Civ. Eng.*, **17**(1), 192-201. https://doi.org/10.1007/s12205-013-1606-0.
Limkatanyu, S., Sae-Long, W., Prachasaree, W. and Kwon, M. (2015b), "Improved nonlinear displacement-based beam element on a two-parameter foundation", *Eur. J. Environ. Civ. Eng.*, **19**(6), 649-671. https://doi.org/10.1080/19648189.2014.965847.
Mindlin, R.D. (1936), "Force at a point in the interior of a semi-infinite solid", *Phys.*, **7**(5), 195-202. https://doi.org/10.1063/1.1745385.
Mullapudi, R. and Ayoub, A. (2010), "Nonlinear finite element modeling of beams on two-parameter foundations", *Comput. Geotech.*, **37**(3), 334-342. https://doi.org/10.1016/j.compgeo.2009.11.006.
Neuenhofer, A. and Filippou, F.C. (1997), "Evaluation of nonlinear frame finite-element models", *J. Struct. Eng.*, **123**(7), 958-966. https://doi.org/10.1061/(ASCE)0733-9445(1997)123:7(958).
Pasternak, P.L. (1954), *On a New Method of Analysis of an Elastic Foundation by means of Two Constants*, Gosudarstvennoe Izdatelstvo Literaturi po Stroitelstvu I Arkhitekture, Moscow, Russia.
Patil, V.A., Sawant, V.A. and Deb, K. (2012), "Finite element analysis of rigid pavement on a nonlinear two parameter foundation model", *Int. J. Geotech. Eng.*, **6**(3), 275-286. https://doi.org/10.3328/IJGE.2012.06.03.274-286.
Raychowdhury, P. and Jindal, S. (2014), "Shallow foundation response variability due to soil and model parameter uncertainty", *Front. Struct. Civ. Eng.*, **8**(3), 237-251. https://doi.org/10.1007/s11709-014-0242-1.
Salari, M.R., Spacone, E., Shing, P.B. and Frangopol, D.M. (1998), "Nonlinear analysis of composite beams with deformable shear connections", *J. Struct. Eng.*, **124**(10), 1148-1158. https://doi.org/10.1061/(ASCE)0733-9445(1998)124:10(1148).
Sapountzakis, E.J. and Kampitsis, A.E. (2013), "Inelastic analysis of beams on two-parameter tensionless elastoplastic foundation", *Eng. Struct.*, **48**, 389-401. https://doi.org/10.1016/j.engstruct.2012.09.012.
Selvadurai, A.P.S. (1979), *Elastic Analysis of Soil-Foundation Interaction*, Elsevier Publishing Company, Inc., New York, U.S.A.
Shirima, L.M. and Giger, M.W. (1992), "Timoshenko beam element resting on two-parameter elastic foundation", *J. Eng. Mech.*, **118**(2), 280-295. https://doi.org/10.1061/(ASCE)0733-9399(1992)118:2(280).
Shokrieh, M.M. and Heidari-Rarani, M. (2011), "A comparative study for beams on elastic foundation models to analysis of mode I delamination in DCB specimen", *Struct. Eng. Mech.*, **37**(2), 149-162. https://doi.org/10.12989/sem.2011.37.2.149.
Spacone, E., Filippou, F.C. and Taucer, F.F. (1996a), "Fiber beam-column model for nonlinear analysis of r/c frames. Part I: Formulation", *Earthq. Eng. Struct. Dyn.*, **25**(7), 711-725. https://doi.org/10.1002/(SICI)1096-9845(199607)25:7<711::AID-EQE576>3.0.CO;2-9.
Spacone, E., Filippou, F.C. and Taucer, F.F. (1996b), "Fiber beam-column model for nonlinear analysis of r/c frames. Part II: Applications", *Earthq. Eng. Struct. Dyn.*, **25**(7), 727-742. https://doi.org/10.1002/(SICI)1096-9845(199607)25:7<727::AID-EQE577>3.0.CO;2-O.
Taylor, R.L. (2000), *FEAP: A Finite Element Analysis Program, User manual: version 7.3*, University of California, Berkeley, California, U.S.A.

Teodoru, I.B. and Musat, V. (2010), "The modified Vlasov foundation model: An attractive approach for beams resting on elastic supports", *Electron. J. Geotech. Eng.*, **15**(C), 1-13.

Tonti, E. (1976), "The reason for analogies between physical theories", *Appl. Math. Modell.*, **1**(1), 37-50. https://doi.org/10.1016/0307-904X(76)90023-8.

Vlasov, V.Z. and Leontiev, U.N. (1966), *Beams, plates, and shells on elastic foundations*, Israel Program for Scientific Translations Ltd, Jerusalem, Israel.

Winkler, E. (1867), *Theory of Elasticity and Srength*, Dominicus, Prague, Czechoslovakia.

Wolfram, S. (1992), *Mathematica Reference Guide*, Addison-Wesley Publishing Company, Redwood City, California, U.S.A.

Zarepour, M., Hosseini, S.A. and Kokaba, M.R. (2017), "Electro-thermo-mechanical nonlinear free vibration of nanobeam resting on the Winkler-Pasternak foundations based on nonlocal elasticity using differential transform method", *Microsyst. Technol.*, **23**(7), 2641-2648. https://doi.org/10.1007/s00542-016-2935-y.

Zendaoui, A., Kadid, A. and Yahiaoui, D. (2016), "Comparison of different numerical models of RC elements for predicting the seismic performance of structures", *Int. J. Concr. Struct. Mater.*, **10**(4), 461-478. https://doi.org/10.1007/s40069-016-0170-7.

Zhang, L., Zhao, M., Zou, X. and Zhao, H. (2009), "Deformation analysis of geocell reinforcement using Winkler model", *Comput. Geotech.*, **36**(6), 977-983. https://doi.org/10.1016/j.compgeo.2009.03.005.

Zhaohua, F. and Cook, R.D. (1983), "Beam elements on two-parameter elastic foundations", *J. Eng. Mech.*, **109**(3), 1390-1401. https://doi.org/10.1061/(ASCE)0733-9399(1983)109:6(1390).

JS

Appendix: Force shape functions

The expression for beam-section force shape function in matrices $\mathbf{N}_{BB}(x)$ and $\mathbf{N}_{BF}(x)$ of Eq. (38) can be expressed as:

$$\begin{aligned}
\mathbf{N}_{BB}(x) &= \begin{bmatrix} N_{BB}^1(x) & N_{BB}^2(x) & N_{BB}^3(x) & N_{BB}^4(x) \end{bmatrix} \\
\mathbf{N}_{BF}(x) &= \begin{bmatrix} N_{BF}^1(x) & N_{BF}^2(x) & N_{BF}^3(x) & N_{BF}^4(x) & N_{BF}^5(x) & N_{BF}^6(x) \end{bmatrix}
\end{aligned} \tag{A1}$$

where

$$\begin{aligned}
&N_{BB}^1(x) = \frac{(L-x)x(15L^3 - 37L^2x + 99Lx^2 + 27x^3)}{15L^4}; \\
&N_{BB}^2(x) = -\frac{(L-x)(L+3x)(L^2 - 2Lx + 3x^2)}{L^4}; \\
&N_{BB}^3(x) = \frac{(L-x)x^2(8L^2 - 36Lx + 27x^2)}{15L^4}; N_{BB}^4(x) = \frac{(2L-3x)^2x^2}{L^4}; \\
&N_{BF}^1(x) = -\frac{(L-x)x^2(8L^2 + 9Lx + 27x^2)}{60L^3}; N_{BF}^2(x) = \frac{(L-3x)(L-x)x^2}{L^2}; \\
&N_{BF}^3(x) = \frac{(L-x)x^2(2L^2 + 21Lx - 27x^2)}{20L^3}; \\
&N_{BF}^4(x) = -\frac{(L-x)x(4L^2 - 9Lx + 9x^2)}{4L^3}; \\
&N_{BF}^5(x) = \frac{3x^2(-L+x)}{L^2}; N_{BF}^6(x) = \frac{3(5L-9x)(L-x)x^2}{4L^3}
\end{aligned} \tag{A2}$$

The expression for foundation-force shape function in matrices $\mathbf{N}_{FB}(x)$ and $\mathbf{N}_{FF}(x)$ of Eq. (36) can be expressed as:

$$\begin{aligned}
\mathbf{N}_{FB}(x) &= \begin{bmatrix} N_{FB}^1(x) & 0 & N_{FB}^1(x) & 0 \\ N_{FB}^2(x) & -N_{FB}^1(x) & N_{FB}^3(x) & -N_{FB}^1(x) \end{bmatrix} \\
\mathbf{N}_{FF}(x) &= \begin{bmatrix} N_{FF}^1(x) & N_{FF}^2(x) & N_{FF}^3(x) & 0 & 0 & 0 \\ N_{FF}^4(x) & N_{FF}^5(x) & \dfrac{N_{FF}^5(x)}{10} & N_{FF}^1(x) & N_{FF}^2(x) & N_{FF}^3(x) \end{bmatrix}
\end{aligned} \tag{A3}$$

where

$$\begin{aligned}
&N_{FB}^1(x) = \frac{4(L-3x)(2L-3x)x}{L^4}; N_{FB}^2(x) = \frac{52(L-3x)(2L-3x)x}{15L^3}; \\
&N_{FB}^3(x) = -\frac{8(L-3x)(2L-3x)x}{15L^3}; N_{FF}^1(x) = \frac{(L-3x)(2L-3x)(L-2x)}{2L^3}; \\
&N_{FF}^2(x) = \frac{3(2L-3x)x}{L^2}; N_{FF}^3(x) = -\frac{3(5L-6x)(L-3x)x}{2L^3}; \\
&N_{FF}^4(x) = -\frac{11(L-3x)(2L-3x)x}{30L^2}; N_{FF}^5(x) = -\frac{(L-3x)(2L-3x)x}{L^2}
\end{aligned} \tag{A4}$$